

# Quantifying linear dune morphology: Examples with SRTM, GDEM, and multibeam bathymetry

Peter L. Guth

Department of Oceanography  
United States Naval Academy  
Annapolis, MD 21402 USA  
pguth@usna.edu

**Abstract**—An automated routine can extract dune crest locations, heights, and wavelength from digital elevation models. The algorithm extracts the fabric from the DEM, draws profiles perpendicular to the crests, and computes statistics from the profiles. Results from the SRTM and ASTER GDEM produce similar results for dunes with heights from 20-100 m and wavelengths of 900-2200 m, and multibeam bathymetry can extract 0.5 m high megaripples with a wavelength of 25 m. In desert regions the ASTER GDEM appears to have few of the anomalies that detract from its performance elsewhere, and provides an improvement over the results with SRTM.

This study will compare periodic landforms extracted from SRTM and GDEM to assess the ability to automatically extract wavelengths, heights, and dune crest positions from DEMs. Finally, to compare the effect of scale on the algorithm, I will look at bedforms extracted from multibeam bathymetry. The natural comparison would be to LIDAR or IFSAR dunes, but I am unaware of a free DEM from those technologies showing linear dunes. The best free high resolution DEM data, 1/3" and 1/9" NED, does not have good data over a dune field comparable to those discussed here.

## INTRODUCTION

Digital elevation models (DEMs) at a range of scales allow quantitative measurement of the earth's surface topography. Wind and water transport can create regular, repetitive landforms, generally called dunes on land and waves, dunes, megaripples, and ripples under water. Despite similarities in shape, different processes can create these bedforms, and multiple scales of periodic forms can occur in the same area [1]. DEMs at the appropriate scale can capture these features, and separate their effects [2].

The Shuttle Radar Topography Mission (SRTM) produced a near global DEM with 3 arc second (3") spacing (~ 90 m) [3]. Because data collection took place in under two weeks, SRTM provides a consistent snapshot of earth's topography; marred only by data voids, largely in mountainous areas and sandy deserts. The use of radar for SRTM removes the effect of weather and clouds. The ASTER GDEM [4] used stereo VNIR imagery collected over almost a decade to create a global DEM with 1" spacing (~ 30 m). GDEM has a number of challenges for DEM users [4], [5], [6], [7], and undetected or incompletely detected clouds contribute significantly. For dynamic topography, potentially including desert dunes, GDEM could show a blurred average in contrast to the single snapshot from SRTM.

## METHODS AND DATA

### *SRTM and ASTER GDEM Data*

DEMs for the complex linear dunes [8] in the Namib Desert came from the ASTER GDEM and the Hydrosheds hole-filled version of SRTM [9]. Computations correctly used the DEMs in their original form with geographic coordinates, without reinterpolation to UTM with subsequent changes to terrain properties and computed statistics. The GDEM has spacing of 1" (about 28.2 x 30.8 m at this latitude), and the SRTM has spacing of 3" (about 84.6 x 92.3 m). Both have elevations stored as integer meters, which can lead to anomalies in analysis in flatter regions (such as small dunes in western Australia).

### *Multibeam Data*

The multibeam grid and sidecan mosaics have a spacing of 0.1667", about 3x5 m for the North Sea. The data was collected with a Klein 5000 sidescan sonar and a SIMRAD EM121A multibeam bathymetric sonar by USNS *Henson* in September 2010. The survey lines ran 140° and 320°, approximately aligned with the tidal currents at 160° and 340°. Tidal currents can reach 0.7 m/sec with two floods and two ebbs daily. Depths in the area range from 60-65 m.

**Methodology**

The methodology requires several parameters, which depend on the scale of both the DEM and the land surface. The same values of the parameters work with GDEM and SRTM in the Namib desert, but the North Sea bathymetry requires different parameters. After the initial setting (or verification) of these parameters, the procedure is designed to run automatically to determine dune height and wavelength, and extract the dune crests.

The first processing step removes a first order (linear) trend surface from the DEM. This places the average elevation at zero. This step could be skipped, or more complicated trend surfaces could be used if the regional geology formed a dome. Figure 1 shows the de-trended ASTER GDEM, with all the dune crests at similar elevations. Figure 2 shows a profile through the DEM.

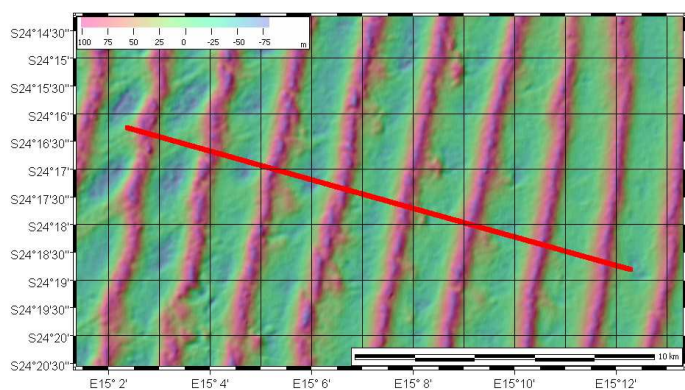


Figure 1. Linear dunes near Sossusvlei, Namibia. Profile line in Fig. 2. shown.

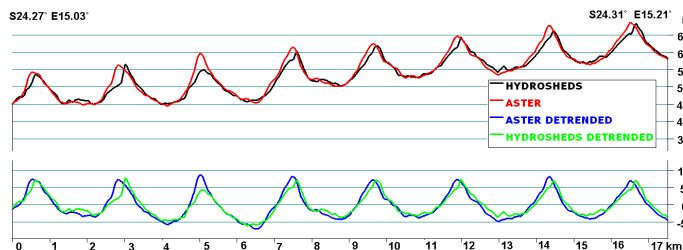


Figure 2. Profiles through dunes with SRTM and GDEM.

The second step extracts the characteristic spacing from the DEM. This could use a number of techniques, two of which are illustrated in Fig. 3 for two points, one on a dune crest and the other between crests. The characteristic spacing occurs when graphs of the parameter level out, indicating no further changes as the spacing increases further. For both locations, the relief plateaus at about 150 m at a distance of 2000 m. The plateau for organization (S2S3, from the terrain organization parameters)

[10] occurs at a value of about 2, but the two locations show a different trend because over shorter distances the crests show stronger organization than the inter-crest regions. This size would be the smallest region size that should be used (it corresponds closely with the dune spacing), and Nyquist sampling theory suggests that regions twice the characteristic wavelength would provide better statistics.

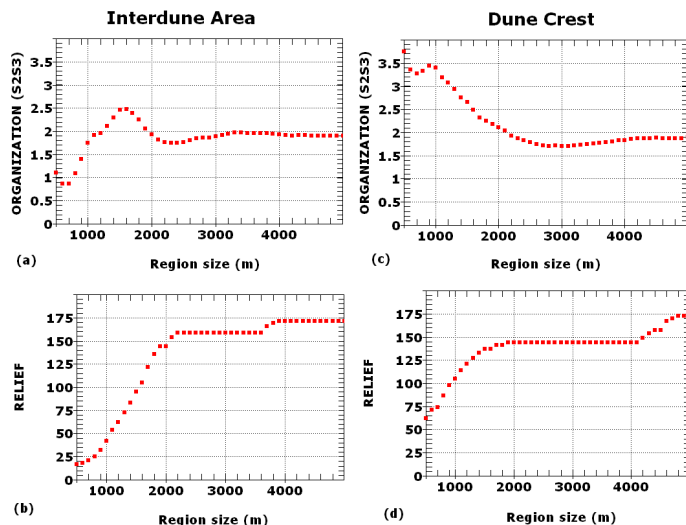


Figure 3. Landform scale from the terrain organization and relief.

The third step computes terrain fabric [10] at selected locations (Fig. 4). This uses the region size computed in step two, and returns a flatness value (S1S2), an organization value (S2S3), and the compass orientation of the ridges. The flatness and organization values can be used as thresholds to define organized regions, since the method does not perform well in flat regions and very low S2S3 values reflect random terrain.

The program can now draw terrain profiles, automatically computing fabric orientation and placing profiles perpendicular to dune crests, and compute dune characteristics (median, mean, and standard deviation for height and length). The computation requires several parameters: (1) profile length; (2) minimum height for a crest from adjacent troughs; (3) closest horizontal spacing for two crests (otherwise only the higher will be selected); and (4) minimum number of identified peaks to allow computation of statistics. The statistics can be displayed, or stored in a database for drawing maps showing spatial distributions of dune characteristics. Table 1 shows statistics for the profiles in Fig. 2, with SRTM and GDEM with both the original DEMs and the de-trended versions.

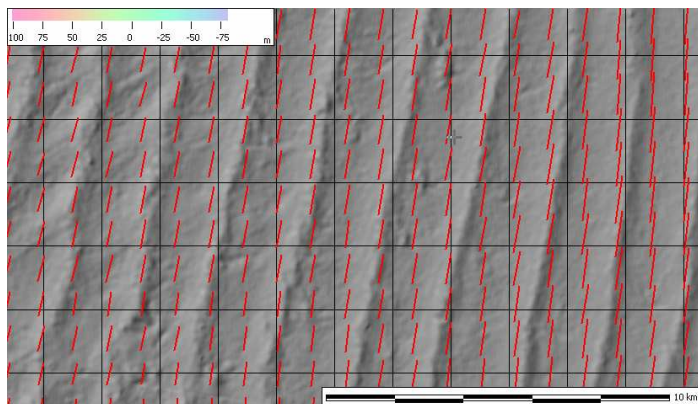


Figure 4. Fabric vectors plotted every 500 m, with a region size of 5000 m.

The algorithm can locate the crest in the profile, and connect them on the map. It starts with the crests identified along a profile, considering each crest in turn. From the first point, the algorithm computes the crest orientation, proceeds a set distance in that direction along the crest, and in case the crest orientation changes, finds the actual crest location by drawing a perpendicular profile to locate the crest. It proceeds to the edge of the map, and then repeats the process in the other direction. The crest can also terminate when the relief between the crest on the trough becomes less than the specified threshold.

TABLE I. DUNE STATISTICS ALONG PROFILE IN FIG. 2

DEM	Wave length (m)			Height (m)		
	Median	Mean	Std Dev	Median	Mean	Std Dev
ASTER	2151	2064	662	119	114	33
ASTER detrend	1857	1899	699	114	119	39
SRTM	1991	2002	633	102	97	34
SRTM detrend	2079	2001	644	105	96	33

## RESULTS

### Desert dunes

The ASTER and SRTM generally performed very similarly (Fig.2, Table 1), although ASTER records higher dune heights. This should not be surprising, and in fact both DEMs probably underpredict the actual dune heights. The algorithm can extract dune crests, and compute the heights and dune spacing throughout the dune fields. Although not reported here, the algorithm also computes dune asymmetry.

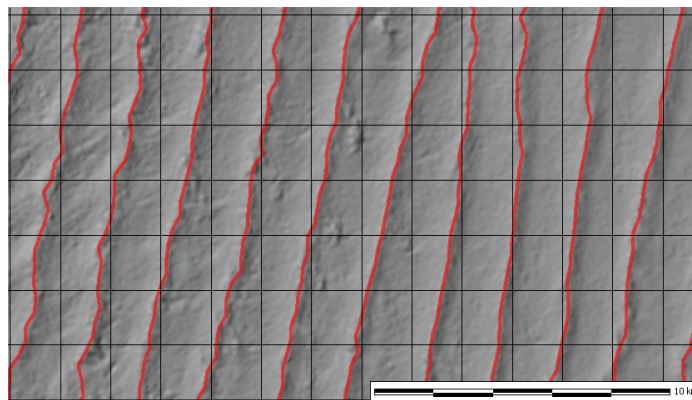


Figure 5. Crests identified automatically.

### Seafloor megaripples

Fig. 6 and 7 show the seafloor in the North Sea from the sidescan sonar and multibeam bathymetry. The computed topographic fabric shows two distinct populations: bedrock ridges, up to 7-8 m above the seafloor, trend about 155-335°, slightly oblique to both the tide and the survey lines. While several of these ridges occur, they show no periodicity. Fig. 8 shows a profile through the multibeam data, with megaripple crests and troughs picked by the algorithm. The mean wavelength is 28.24 m, with a standard deviation of 16.88 and a median of 24.50 m. The mean height is 0.44 m, with a standard deviation of 0.23 and a median of 0.43 m.

## CONCLUSION

In addition to the work presented here, I have looked at dunes in Australia, China, Afghanistan, Saudi Arabia, Egypt, Niger, and Algeria with both GDEM and SRTM. The smallest dunes (in Australia) had wavelengths of 920 m and heights of 19 m, and while this is close to the resolution limits for GDEM (Hugenholz and Barchyn [2] reported that GDEM could not resolve the smallest dunes, generally < 15 m tall, in the Badain Jaran Desert of China) the algorithm performed satisfactorily. Some anomalies appeared in the GDEM, most obviously in China and the flat terrain in Australia, but it appears that GDEM performs much better in desert regimes compared to problems elsewhere, probably due to the lack of clouds.

Given an appropriate DEM, it appears possible to extract dune field parameters over a range of scales, both in the terrain and the source DEM. With the release of GDEM version 2 expected in summer 2011, this will allow a global inventory of linear dunes, and the extension of the algorithm to more complex dunes.

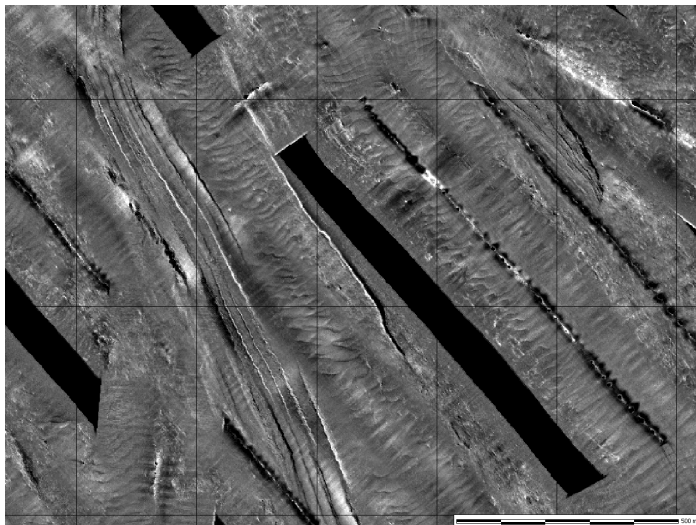


Figure 6. Sidescan sonar mosaic

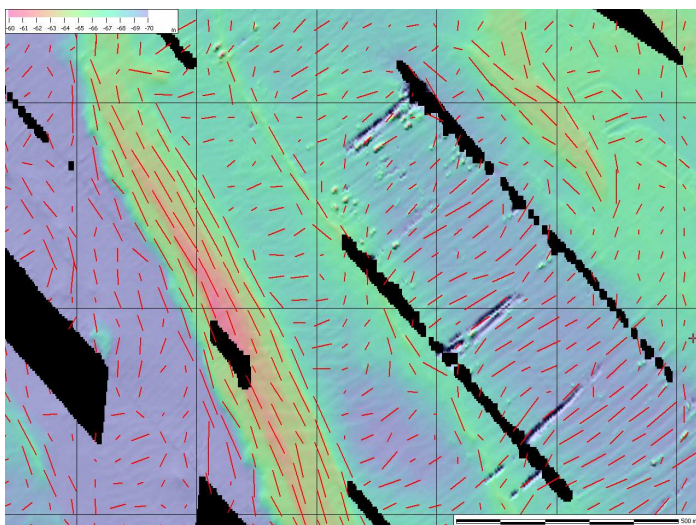


Figure 7. Multibeam bathymetry, with seafloor fabric show with red vectors.

ACKNOWLEDGMENT

I thank the providers of the DEM data which made possible this comparison: (1) The Ministry of Economy, Trade and Industry of Japan (METI) and the National Aeronautics and Space Administration (NASA) for ASTER GDEM; (2) the National Geospatial-Intelligence Agency (NGA) and NASA for the SRTM, and CGIAR-CSI and the World Wildlife Foundation (WWF) for their hole filling programs; and (3) the Naval

Oceanographic Office for the multibeam bathymetry. This study used the MICRODEM program [11].

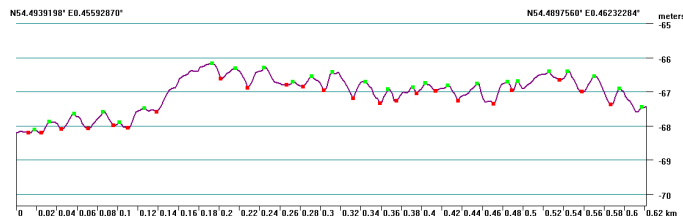


Figure 8. Topographic profile perpendicular to megaripple crests.

REFERENCES

[1] Dong, Z., Qian, G., Luo, W., Zhang, Z., Xiao, S., and Zhao A., 2009. "Geomorphological hierarchies for complex mega-dunes and their implications for mega-dune evolution in the Badain Jaran Desert." *Geomorphology*, 106, 180–185.

[2] Hugenholtz, C.H., and Barchyn T.E., 2010. "Spatial analysis of sand dunes with a new global topographic dataset: new approaches and opportunities." *Earth Surface Processes and Landforms*, 35(8), 986-992.

[3] Farr, T.G., Rosen, P.A., Caro, E., and 15 others, 2007. "The shuttle radar topography mission": *Reviews of Geophysics*: 45(2): RG2004, doi:10.1029/2005RG000183.

[4] Abrams, M., Bailey, B., Tsu, H., and Hato, M., 2010. "The ASTER global DEM": *Photogrammetric Engineering & Remote Sensing*, 76(4), pp.344-348.

[5] Slater, J.A., Heady, B., Kroenung, G., Curtis, W., Haase, J., Hoegemann, D., Shockley, C., and Tracy, Kevin, 2011. "Global assessment of the new ASTER Global Digital Elevation Model": *Photogrammetric Engineering & Remote Sensing*, 77(4), p.335-349.

[6] Guth, P.L., 2010, Geomorphometric Comparison of ASTER GDEM and SRTM: ASPRS/CaGIS 2010 Fall Specialty Conference, Orlando, FL, November 15-19, 10 page paper on Conference CD-ROM.

[7] Hengl, T., and Reuter, H.I., 2011, "How accurate and usable is GDEM? A statistical assessment of GDEM using LiDAR data." In *Geomorphometry 2011*, edited by T. Hengl, I. S. Evans, J. P. Wilson and M. Gould, 45-48. Redlands, CA, 2011.

[8] Livingstone, I., Bristow, C., Bryant, R.G., Bullard, J., White, K., Wiggs, G.F.S., Baas, A.C.W., Bateman, M.D., and Thomas, D.S.G., 2010. "The Namib Sand Sea Digital Database of aeolian dunes and key forcing variables". *Journal of Aeolian Research*, 2 (2-3), 93-104.

[9] Lehner, B., Verdin, K., and Jarvis, J, 2008. New global hydrography derived from spaceborne elevation data: *EOS*, 89, 93-94

[10] Guth, P.L., 2001. "Quantifying terrain fabric in digital elevation models", in Ehlen, J., and Harmon, R.S., eds., *The environmental legacy of military operations*, Geological Society of America *Reviews in Engineering Geology*, 14, 13-25.

[11] Guth, P.L., 2009. "Geomorphometry in MICRODEM", In Hengl, T., Reuter, H.I. (eds), *Geomorphometry: concepts, software, applications. Developments in Soil Science Series*, Elsevier, pp.351-366.